MOT Solution of the PMCHWT Equation for Analyzing Transient Scattering from Conductive Dielectrics

Ismail E. Uysal, *Student Member, IEEE*, H. Arda Ülkü, *Member, IEEE*, and Hakan Bağcı, *Senior Member, IEEE*

***Abstract*—Transient electromagnetic interactions on conductive dielectric scatterers are analyzed by solving the Poggio–Miller–Chan–Harrington–Wu–Tsai (PMCHWT) surface integral equation with a marching on-in-time (MOT) scheme. The proposed scheme, unlike the previously developed ones, permits the analysis on scatterers with multiple volumes of different conductivity. This is achieved by maintaining an extra temporal convolution that only depends on permittivity and conductivity of these volumes. Its discretization and computation come at almost no additional cost and do not change the computational complexity of the resulting MOT solver. Accuracy and applicability of the MOT-PMCHWT solver are demonstrated by numerical examples.**

***Index Terms*—Conductive media, dissipative media, integral equations, lossy media, marching-on-in-time method, PMCHWT formulation, time-domain analysis, transient analysis.**

I. Introduction

TIME-DOMAIN surface integral equation (TDSIE) solvers have been used extensively for analyzing transient scattering from highly realistic objects involving perfect electrically conducting (PEC) surfaces, lossless dielectric bodies, and thin wires, all of which reside in a lossless unbounded space [1]. However, their application to lossy dielectric and PEC scatterers residing in a lossy/dispersive medium has been very limited [2]–[6]. This is simply due to the fact that Green function of such a medium has a temporal tail [7]. Consequently, computation of the convolution of the Green function and currents becomes very costly, and the resulting marching-on-in-time (MOT)-based TDSIE solvers have to be accelerated using blocked fast Fourier transform (blocked-FFT) [3], plane-wave time domain (PWTD) [4], and/or Prony-series [5], [6] schemes.

The first MOT scheme [2] developed for lossy dielectrics solves four coupled TDSIEs constructed in tangential and normal components of the fields on the interface between the lossy scatterer and the lossless background medium. Because of the "operator scaling" introduced in the equations to eliminate a temporal convolution, this scheme cannot be directly applied to scatterers with volumes of different conductivity. In [6], an MOT scheme for solving the electric field SIE enforced on interfaces between volumes of different conductivity is proposed. However, this scheme suffers from the problem of interior resonances if any one of the volumes is lossless [8].

In this letter, a more general MOT-TDSIE scheme is proposed for characterizing transient electromagnetic interactions on lossy dielectrics. The proposed scheme solves the time-domain extension of the Poggio–Miller–Chan–Harrington–Wu–Tsai (PMCHWT) SIE for the tangential components of the electric and magnetic fields on the interfaces between dielectric volumes. The unknowns are discretized using the Rao–Wilton–Glisson (RWG) basis functions [9] in space and Lagrange polynomials [10] in time. Contributions of this work are twofold: 1) the proposed MOT scheme can directly be applied to scatterers with volumes of different conductivity and does not have the interior resonance problem (incase any one of the volumes is lossless) since it uses the PMCHWT formulation; 2) the time domain PMCHWT SIE has a convolution term that involves the complex permittivity's inverse Fourier transform, Green function, and charge density. This term is discretized into a double discrete summation where the inner summation corresponds to the convolution of the Green function and basis functions. The multipliers in the outer summation depend only on the conductivity and permittivity, therefore they are precomputed per medium without introducing any significant computational burden. For unaccelerated MOT schemes, the multipliers in the outer summation are simply combined with the matrix entries resulting from the convolution of the Green function and basis functions. For FFT- or PWTD-accelerated MOT schemes [3], [4], the outer summation is computed efficiently using blocked-FFTs [11].

II. Formulation

A. Time-Domain PMCHWT SIE

Let $V = \bigcup_{p=0}^{M} V_p$ represent the total volume of a composite scatterer consisting of M number of isotropic, homogeneous, and conductive regions. Volume, permittivity, permeability, and conductivity of these regions are denoted by V_p, ε_p, μ_p, and

Manuscript received October 10, 2014; revised November 05, 2014; accepted November 10, 2014. Date of publication November 11, 2014; date of current version February 06, 2015.

I. E. Uysal is with the Division of Computer, Electrical, and Mathematical Sciences and Engineering (CEMSE), King Abdullah University of Science and Technology (KAUST), Thuwal 23955-6900, Saudi Arabia (e-mail: ismail.uysal@kaust.edu.sa).

H. A. Ülkü is with the Division of Computer, Electrical, and Mathematical Sciences and Engineering (CEMSE), King Abdullah University of Science and Technology (KAUST), Thuwal 23955-6900, Saudi Arabia, and also with the Department of Electronics Engineering, Gebze Institute of Technology, Kocaeli 41400, Turkey (e-mail: huseyin.ulku@kaust.edu.sa; haulku@gyte.edu.tr).

H. Bağcı is with the Division of Computer, Electrical, and Mathematical Sciences and Engineering (CEMSE) and Center for Uncertainty Quantification in Computational Science and Engineering, King Abdullah University of Science and Technology (KAUST), Thuwal 23955-6900, Saudi Arabia (e-mail: hakan.bagci@kaust.edu.sa).

Color versions of one or more of the figures in this letter are available online at http://ieeexplore.ieee.org.

Digital Object Identifier 10.1109/LAWP.2014.2369829

1536-1225 © 2014 IEEE. Translations and content mining are permitted for academic research only. Personal use is also permitted, but republication/redistribution requires IEEE permission. See http://www.ieee.org/publications_standards/publications/rights/index.html for more information.

σ_p, respectively. The surface of interface between regions p and q is represented by S_{pq}, $p, q = 1, \ldots, N$, $p \neq q$, and $\hat{\mathbf{n}}_{pq}(\mathbf{r})$ is the unit normal vector on S_{pq} pointing toward V_p. Note that $S_{pq} = S_{qp}$ and $\hat{\mathbf{n}}_{pq}(\mathbf{r}) = -\hat{\mathbf{n}}_{qp}(\mathbf{r})$. Let $\mathbf{E}_p^{\text{inc}}(\mathbf{r}, t)$ and $\mathbf{H}_p^{\text{inc}}(\mathbf{r}, t)$ denote the incident electric and magnetic fields due to a source located in V_p. It is assumed that $\mathbf{E}_p^{\text{inc}}(\mathbf{r}, t)$ and $\mathbf{H}_p^{\text{inc}}(\mathbf{r}, t)$ are zero $\forall \mathbf{r} \in V_p$, $t < 0$ and band-limited to $f_{\max}$. Upon excitation, equivalent electric and magnetic current densities $\mathbf{J}_{pq}(\mathbf{r}, t)$ and $\mathbf{M}_{pq}(\mathbf{r}, t)$ are induced on S_{pq}. Note that $\mathbf{J}_{pq}(\mathbf{r}, t) = -\mathbf{J}_{qp}(\mathbf{r}, t)$ and $\mathbf{M}_{pq}(\mathbf{r}, t) = -\mathbf{M}_{qp}(\mathbf{r}, t)$. PMCHWT SIE is obtained using surface equivalence principles and boundary conditions [12]

$$\begin{aligned}
&\hat{\mathbf{n}}_{pq}(\mathbf{r}) \times \partial_t \mathbf{E}_p^{\text{inc}}(\mathbf{r}, t) + \hat{\mathbf{n}}_{qp}(\mathbf{r}) \times \partial_t \mathbf{E}_q^{\text{inc}}(\mathbf{r}, t) \\
&\quad = -\hat{\mathbf{n}}_{pq}(\mathbf{r}) \times \sum_{p'} [\mathcal{L}_p\{\mathbf{J}_{pp'}(\mathbf{r}, t)\} - \mathcal{K}_p\{\mathbf{M}_{pp'}(\mathbf{r}, t)\}] \\
&\qquad - \hat{\mathbf{n}}_{qp}(\mathbf{r}) \times \sum_{q'} [\mathcal{L}_q\{\mathbf{J}_{qq'}(\mathbf{r}, t)\} - \mathcal{K}_q\{\mathbf{M}_{qq'}(\mathbf{r}, t)\}] \quad (1)
\end{aligned}$$

$$\begin{aligned}
&\hat{\mathbf{n}}_{pq}(\mathbf{r}) \times \partial_t \mathbf{H}_p^{\text{inc}}(\mathbf{r}, t) + \hat{\mathbf{n}}_{qp}(\mathbf{r}) \times \partial_t \mathbf{H}_q^{\text{inc}}(\mathbf{r}, t) \\
&\quad = -\hat{\mathbf{n}}_{pq}(\mathbf{r}) \times \sum_{p'} [\mathcal{P}_p\{\mathbf{M}_{pp'}(\mathbf{r}, t)\} + \mathcal{K}_p\{\mathbf{J}_{pp'}(\mathbf{r}, t)\}] \\
&\qquad - \hat{\mathbf{n}}_{qp}(\mathbf{r}) \times \sum_{q'} [\mathcal{P}_q\{\mathbf{M}_{qq'}(\mathbf{r}, t)\} + \mathcal{K}_q\{\mathbf{J}_{qq'}(\mathbf{r}, t)\}]. \quad (2)
\end{aligned}$$

The integral operators $\mathcal{L}_p\{\cdot\}$, $\mathcal{K}_p\{\cdot\}$, and $\mathcal{P}_p\{\cdot\}$ are

$$\begin{aligned}
\mathcal{L}_p\{\mathbf{X}_{pp'}(\mathbf{r}, t)\} &= -\mu_p \mathcal{V}_p\{\partial_t \mathbf{X}_{pp'}(\mathbf{r}, t)\} + \frac{1}{\varepsilon_p} \mathcal{Q}_p\{\mathbf{X}_{pp'}(\mathbf{r}, t)\} \\
&\quad - \mathcal{Q}_p\{\gamma_p(t) * \mathbf{X}_{pp'}(\mathbf{r}, t)\} \quad (3)
\end{aligned}$$

$$\begin{aligned}
\mathcal{P}_p\{\mathbf{X}_{pp'}(\mathbf{r}, t)\} &= -\varepsilon_p \mathcal{V}_p\{\partial_t \mathbf{X}_{pp'}(\mathbf{r}, t)\} + \frac{1}{\mu_p} \mathcal{Q}_p\{\mathbf{X}_{pp'}(\mathbf{r}, t)\} \\
&\quad - \sigma_p \mathcal{V}_p\{\mathbf{X}_{pp'}(\mathbf{r}, t)\} \quad (4)
\end{aligned}$$

$$\mathcal{K}_p\{\mathbf{X}_{pp'}(\mathbf{r}, t)\} = \nabla \times \mathcal{V}_p\{\mathbf{X}_{pp'}(\mathbf{r}, t)\} \quad (5)$$

where

$$\mathcal{V}_p\{\mathbf{X}_{pp'}(\mathbf{r}, t)\} = \int_{S_{pp'}} g_p(R, t) * \partial_t \mathbf{X}_{pp'}(\mathbf{r}', t) ds' \quad (6)$$

$$\mathcal{Q}_p\{\mathbf{X}_{pp'}(\mathbf{r}, t)\} = \nabla \int_{S_{pp'}} g_p(R, t) * \nabla' \cdot \mathbf{X}_{pp'}(\mathbf{r}', t) ds'. \quad (7)$$

Here, $g_p(R, t)$ is the Green function of the unbounded medium with the same material properties as V_p, $R = |\mathbf{r} - \mathbf{r}'|$ is the distance between the observer and source points $\mathbf{r}$ and $\mathbf{r}'$, and ∂_t and $*$ denote the temporal derivative and convolution, respectively. $g_p(R, t)$ is computed using [7]

$$\begin{aligned}
g_p(R, t) &= \frac{e^{-bt}}{4\pi R} \delta(\tau) + g_p^{\text{tail}}(R, t) \\
g_p^{\text{tail}}(R, t) &= \frac{b e^{-bt}}{4\pi c_p} \frac{I_1(ba)}{a} u(\tau) \quad (8)
\end{aligned}$$

where $\tau = t - R/c_p$, $c_p = 1/\sqrt{\varepsilon_p \mu_p}$ is the speed of light, $b = \sigma_p/(2\varepsilon_p)$, $a = \sqrt{t^2 - R^2/c_p^2}$, $I_1(\cdot)$ is the first-order modified Bessel function of the first kind, $\delta(\cdot)$ is the Dirac delta function, and $u(\cdot)$ is the unit step function. In (3), $\gamma_p(t)$ is obtained analytically using inverse Fourier transform as

$$\gamma_p(t) = \mathcal{F}^{-1}\left\{\frac{\sigma_p}{\varepsilon_p(\sigma_p + j\omega\varepsilon_p)}\right\} = \frac{\sigma_p}{\varepsilon_p^2} e^{-\frac{\sigma_p t}{\varepsilon_p}} u(t). \quad (9)$$

Several observations about the time-domain PMCHWT SIE in (1) and (2) are in order.

1) Summations over indices p' and q' represent the contribution to the scattered electric and magnetic fields evaluated on S_{pq} from the currents induced on $S_{pp'}$ and $S_{qq'}$ surrounding V_p and V_q, respectively.
2) Equations (1) and (2) are "scaled" with ∂_t to eliminate a time integral that would be present in the operator $\mathcal{Q}_p\{\cdot\}$. It should be noted here that unlike the scaling factor $\partial_t + \sigma/\varepsilon$ used in SIEs formulated in [2] and [3], this operation does not limit the applicability of (1) and (2) to volumes with the same conductivity.
3) Discretization of $\mathcal{Q}_p\{\gamma_p(t) * \mathbf{X}_{pp'}(\mathbf{r}, t)\}$ in (3) requires discretization of two convolutions applied back to back.
4) If $\sigma_p = 0$, then $g_p^{\text{tail}}(R, t) = 0$ and $g_p(R, t) = \delta(\tau)/(4\pi R)$. Additionally, last terms in (3) and (4) vanish since $\gamma_p(t) = 0$ and $\sigma_p = 0$. Consequently, the time-domain PMCHWT SIE in (1) and (2) is reduced to that in [13].

B. Discretization

MOT Scheme: Equivalent surface current densities are expanded using RWG functions $\mathbf{f}_{e'n'}(\mathbf{r})$ [9] in space, where e' refers to the index of S_{pq} and n' is the index of the basis functions on S_{pq}, and shifted Lagrange interpolation functions $T^{j'}(t) = T(t - j'\Delta t)$ [10] in time

$$\mathbf{J}_e'(\mathbf{r}, t) = \sum_{j'=1}^{N_t} \sum_{n'=1}^{N_e} J_{e'n'}^{j'} \mathbf{f}_{e'n'}(\mathbf{r}) T^{j'}(t) \quad (10)$$

$$\mathbf{M}_e'(\mathbf{r}, t) = \sum_{j'=1}^{N_t} \sum_{n'=1}^{N_e} M_{e'n'}^{j'} \mathbf{f}_{e'n'}(\mathbf{r}) T^{j'}(t). \quad (11)$$

Here, $J_{e'n'}^{j'}$ and $M_{e'n'}^{j'}$ are the unknown coefficients, Δt is the time-step size, and N_e and N_t are the numbers of spatial basis functions on S_{pq} and time-steps, respectively. Inserting (10) and (11) into (1) and (2) and testing the resulting equations with $\hat{\mathbf{n}}_{pq}(\mathbf{r}) \times \mathbf{f}_{en}(\mathbf{r}) \delta(t - j\Delta t)$, $e \in S_{pq}$, $n = 1, \ldots, N_e$, result in a system of equations

$$\begin{aligned}
&\sum_{j'=1}^{j} \left\{ \sum_{p'} \alpha_{pp'} \sum_{e' \in S_{pp'}} \sum_{n'} [A_{p,en,e'n'}^{j-j'} J_{e'n'}^{j'} - B_{p,en,e'n'}^{j-j'} M_{e'n'}^{j'}] \right. \\
&\quad \left. - \sum_{q'} \alpha_{qq'} \sum_{e' \in S_{qq'}} \sum_{n'} [A_{q,en,e'n'}^{j-j'} J_{e'n'}^{j'} - B_{q,en,e'n'}^{j-j'} M_{e'n'}^{j'}] \right\} \\
&\quad = E_{pq,en}^{j} \quad (12)
\end{aligned}$$

$$\begin{aligned}
&\sum_{j'=1}^{j} \left\{ \sum_{p'} \alpha_{pp'} \sum_{e' \in S_{pp'}} \sum_{n'} [C_{p,en,e'n'}^{j-j'} M_{e'n'}^{j'} + B_{p,en,e'n'}^{j-j'} J_{e'n'}^{j'}] \right. \\
&\quad \left. - \sum_{q'} \alpha_{qq'} \sum_{e' \in S_{qq'}} \sum_{n'} [C_{q,en,e'n'}^{j-j'} M_{e'n'}^{j'} + B_{q,en,e'n'}^{j-j'} J_{e'n'}^{j'}] \right\} \\
&\quad = H_{pq,en}^{j} \quad (13)
\end{aligned}$$

where

$$E_{pq,en}^{j} = -\left\langle \mathbf{f}_{en}(\mathbf{r}), \partial_t \mathbf{E}_p^{\text{inc}}(\mathbf{r}, t) - \partial_t \mathbf{E}_q^{\text{inc}}(\mathbf{r}, t) \right\rangle_{t = j\Delta t} \quad (14)$$

$$H^{j}_{pq,en} = -\langle \mathbf{f}_{en}(\mathbf{r}), \partial_t \mathbf{H}^{\rm inc}_p(\mathbf{r},t) - \partial_t \mathbf{H}^{\rm inc}_q(\mathbf{r},t)\rangle_{t=j\Delta t} \tag{15}$$

$$A^{j-j'}_{p,en,e'n'} = \left\langle \mathbf{f}_{en}(\mathbf{r}), \mathcal{L}_p\{\mathbf{f}_{e'n'}(\mathbf{r})T^{j'}(t)\}\right\rangle_{t=j\Delta t} \tag{16}$$

$$B^{j-j'}_{p,en,e'n'} = \left\langle \mathbf{f}_{en}(\mathbf{r}), \mathcal{K}_p\{\mathbf{f}_{e'n'}(\mathbf{r})T^{j'}(t)\}\right\rangle_{t=j\Delta t} \tag{17}$$

$$C^{j-j'}_{p,en,e'n'} = \left\langle \mathbf{f}_{en}(\mathbf{r}), \mathcal{P}_p\{\mathbf{f}_{e'n'}(\mathbf{r})T^{j'}(t)\}\right\rangle_{t=j\Delta t}. \tag{18}$$

$\langle \mathbf{f}_{en}(\mathbf{r}), \mathbf{X}(\mathbf{r},t)\rangle = \int_{\Delta_{en}} \mathbf{f}_{en}(\mathbf{r})\cdot\mathbf{X}(\mathbf{r},t)ds$, Δ_{en} is the support of the testing function $\mathbf{f}_{en}(\mathbf{r})$, and $\alpha_{pp'} = \pm 1$ for $p \gtrless p'$. Equations (12) and (13) are brought into a form that can be solved using the well-known MOT scheme [13]

$$\mathbf{Z}_0\mathbf{I}_j = \mathbf{V}_j - \sum_{j'=1}^{j-1} \mathbf{Z}_{j-j'}\mathbf{I}_{j'} \tag{19}$$

where $\mathbf{I}_j$ and $\mathbf{V}_j$ are $N\times 1$ vectors storing the unknown coefficients and tested fields at time-step j and $\mathbf{Z}_{j-j'}$ are the $N\times N$ MOT matrices. Here, $N = 2\sum_{e\in S_{pq}} N_e$, and $\mathbf{V}_j$ and $\mathbf{Z}_{j-j'}$ are constructed by combining the vector and matrix elements in (14)–(15) and (16)–(18), respectively.

Convolutions: The scheme described above requires two types of convolutions to be computed at $t = j\Delta t$ at the testing points.

1) Convolutions of $g_p(R,t)$ with $\mathbf{f}_{e'n'}(\mathbf{r})T^{j'}(t)$ and $\nabla\cdot\mathbf{f}_{e'n'}(\mathbf{r})T^{j'}(t)$ (i.e., $\mathcal{V}_p\{\mathbf{f}_{e'n'}(\mathbf{r})T^{j'}(t)\}_{t=j\Delta t}$ and $\mathcal{Q}_p\{\mathbf{f}_{e'n'}(\mathbf{r})T^{j'}(t)\}_{t=j\Delta t}$). Methods to efficiently compute these convolutions are proposed in [5] and [6] and are not described here.
2) Convolution of $g_p(R,t)$ with $\gamma_p(t)*\nabla\cdot\mathbf{f}_{e'n'}(\mathbf{r})T^{j'}(t)$ (i.e., $\mathcal{Q}_p\{\gamma_p(t)*\mathbf{f}_{e'n'}(\mathbf{r})T^{j'}(t)\}_{t=j\Delta t}$). The method to compute this convolution is one of the contributions of this work and is described next.

This method represents

$$\mathcal{Q}_p\{\gamma_p(t)*\mathbf{f}_{e'n'}(\mathbf{r})T^{j'}(t)\}_{t=j\Delta t} = \left\{\nabla\int_{\Delta_{e'n'}} g_p(R,t)*\gamma_p(t)*\nabla'\cdot\mathbf{f}_{e'n'}(\mathbf{r}')T^{j'}(t)ds'\right\}_{t=j\Delta t} \tag{20}$$

in terms of $\mathcal{Q}_p\{\mathbf{f}_{e'n'}(\mathbf{r})T^{j'}(t)\}_{t=j\Delta t}$ [type-1 convolution], which can be computed efficiently using existing methods [5], [6]. To this end, first, the auxiliary function $F^{j'}_p(t) = \gamma_p(t)*T^{j'}(t)$ is approximated using

$$F^{j'}_p(t) = \sum_{l'=1}^{N_t} \tilde{F}^{j'l'}_p T^{l'}(t) \tag{21}$$

where $\tilde{F}^{j'l'}_p = F^{j'}_p(l'\Delta t) = \gamma_p(t)*T^{j'}(t)|_{t=l'\Delta t}$ are

$$\tilde{F}^{j'l'}_p = \int_{\max([l'-j'-d]\Delta t,0)}^{(l'-j'+1)\Delta t} \gamma_p(t')T([l'-j']\Delta t - t')dt' = \int_{-\Delta t}^{\min(l'-j',d)\Delta t} \gamma_p([l'-j']\Delta t - \tilde{t})T(\tilde{t})d\tilde{t} = \tilde{F}^{l'-j'}_p. \tag{22}$$

Here, $[-\Delta t, d\Delta t]$ and d are the support and order of $T(t)$, respectively. In (22), notation representing $F^{j'}_p(l'\Delta t)$ is changed to $\tilde{F}^{l'-j'}_p$ because they depend only on $l'-j'$. Note that $\tilde{F}^{l'-j'}_p = 0$ for $j' \geq l'+1$. Inserting (21) into (20) yields

$$\mathcal{Q}_p\{\gamma_p(t)*\mathbf{f}_{e'n'}(\mathbf{r})T^{j'}(t)\}_{t=j\Delta t} = \sum_{l'=1}^{j}\tilde{F}^{l'-j'}_p\left\{\nabla\int_{\Delta_{e'n'}} g_p(R,t)*\nabla'\cdot\mathbf{f}_{e'n'}(\mathbf{r}')T^{l'}(t)ds'\right\}_{t=j\Delta t} = \sum_{l'=1}^{j}\tilde{F}^{l'-j'}_p\,\mathcal{Q}_p\{\mathbf{f}_{e'n'}(\mathbf{r})T^{l'}(t)\}_{t=j\Delta t}. \tag{23}$$

This clearly shows that the computation of type-2 convolution $\mathcal{Q}_p\{\gamma_p(t)*\mathbf{f}_{e'n'}(\mathbf{r})T^{j'}(t)\}_{t=j\Delta t}$ is reduced to that of type-1 convolution $\mathcal{Q}_p\{\mathbf{f}_{e'n'}(\mathbf{r})T^{l'}(t)\}_{t=j\Delta t}$. Finally, contribution from fully tested $\mathcal{Q}_p\{\gamma_p(t)*\mathbf{f}_{e'n'}(\mathbf{r})T^{j'}(t)\}$ to $\mathbf{Z}_{j-j'}$ is expressed as

$$\left\langle \mathbf{f}_{en}(\mathbf{r}), \mathcal{Q}_p\{\gamma_p(t)*\mathbf{f}_{e'n'}(\mathbf{r})T^{j'}(t)\}\right\rangle\Big|_{t=j\Delta t} = \sum_{l'=1}^{j}\left\langle \mathbf{f}_{en}(\mathbf{r}), \mathcal{Q}_p\{\mathbf{f}_{e'n'}(\mathbf{r})T^{l'}(t)\}\right\rangle_{t=j\Delta t}\tilde{F}^{l'-j'}_p. \tag{24}$$

Comments: Several comments about the discretization scheme described above are in order.

1) Convolution in (22) depends only on ε_p and σ_p, therefore $\tilde{F}^{l'-j'}_p$ are computed and stored per volume.
2) The cost of evaluating $\tilde{F}^{l'-j'}_p$ is negligible when compared to that of type-1 convolutions. For unaccelerated MOT schemes, the discrete sum in (24) is directly incorporated into the MOT matrices $\mathbf{Z}_{j-j'}$ in (19) with almost no additional cost on computing $\mathbf{Z}_{j-j'}$. The cost of time marching stays exactly the same.
3) For FFT or PWTD-accelerated MOT schemes [3], [4], the discrete summation $\sum_{j'=1}^{l'-1}\tilde{F}^{l'-j'}_p J^{j'}_{e'n'}$ that is present on the right-hand side of (19) can be computed efficiently during time marching using blocked-FFTs [11].

III. Numerical Results

In this section, the accuracy and the applicability of the proposed MOT-PMCHWT solver are demonstrated via analysis of transient scattering from dielectric objects residing in free space. In all examples, the electric field of the incident plane wave is given by $\mathbf{E}^{\rm inc}_0(\mathbf{r},t) = \hat{x}G(t-\hat{z}\cdot\mathbf{r}/c_0)$, where $G(t) = \cos(2\pi f_0[t-t_0])\exp(-[t-t_0]^2/2\sigma^2)$ is a Gaussian pulse with modulation frequency f_0, duration $\sigma = 3/(2\pi f_{\rm bw})$, bandwidth $f_{\rm bw}$, and delay $t_0 = 7.5\sigma$. Excitation exists only in free space denoted as dielectric volume with $p = 0$.

The first example is a layered sphere with inner and outer radius of 0.5 m. The relative permittivity and conductivity in the core and layer are 1.5 and 0.003 S/m and 1.3 and 0.001 S/m. For this simulation, $f_0 = 100$ MHz, $f_{\rm bw} = 75$ MHz, $N = 6054$, $d = 4$, $N_t = 2000$, and $\Delta t = 0.1905$ ns. Fig. 1 plots the coefficients of two basis functions approximating electric and magnetic current densities. Results are stable for the duration of simulation. Fig. 2 compares radar cross section (RCS) results obtained from the MOT solution for $\phi = 0^\circ$ and $0^\circ \leq \theta < 180^\circ$ at 50 and 150 MHz to those obtained using Mie series. Results agree very well.

The second example is a six-layer Luneburg lens [14]. Thicknesses, permittivities, and conductivities of the layers (from inner to outer) are $\{0.39, 0.16, 0.13, 0.10, 0.10, 0.12\}$ mm,

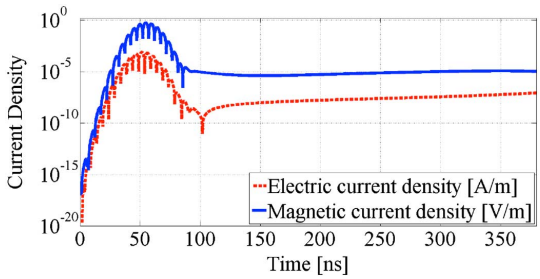

Fig. 1. Coefficients of two basis functions approximating electric and magnetic current densities.

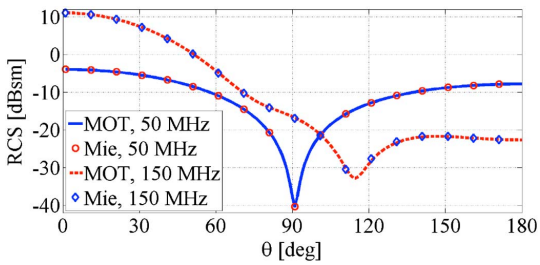

Fig. 2. RCS obtained from the MOT and Mie-series solutions for $\phi = 0°$ and $0° \leq \theta < 180°$ at 50 and 150 MHz.

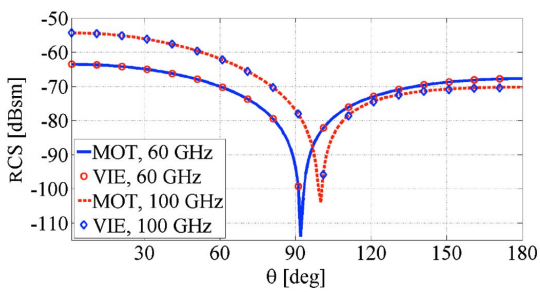

Fig. 3. RCS obtained from the MOT and FD-VIE solutions for $\phi = 0°$ and $0° \leq \theta < 180°$ at 60 and 100 GHz.

$\{1.92, 1.77, 1.62, 1.46, 1.31, 1.05\}$, and $\{0.096, 0.082, 0.071, 0.048, 0.035, 0\}$ S/m, respectively. For this simulation, $f_0 = 80$ GHz, $f_{\rm bw} = 50$ GHz, $N = 7662$, $d = 4$, $N_t = 1000$, and $\Delta t = 0.2564$ ps. Fig. 3 compares RCS results obtained from the MOT and frequency-domain volume integral equation (FD-VIE) solutions for $\phi = 0°$ and $0° \leq \theta < 180°$ at 60 and 100 GHz. Results agree very well.

IV. Conclusion

An MOT scheme, which solves the time-domain PMCHWT SIE for analyzing transient electromagnetic wave interactions on conductive dielectric scatterers, is described. The resulting MOT-PMCHWT solver, unlike previously developed schemes, allows for scatterers with multiple volumes of different conductivity with almost no increase in the computational cost. The accuracy and applicability of the solver is demonstrated by numerical examples.

Development of an MOT-PMCHWT solver for more general dispersive dielectric scatterers is underway.

Appendix

Derivative of $g_p(R,t)$ with respect to R is needed in (17). This is evaluated using

$$\frac{\partial g_p(R,t)}{\partial R} = -\frac{e^{-\frac{b}{c_p}R}}{4\pi R}\left\{\frac{\delta(\tau)}{R} + \frac{b\delta(\tau)}{c_p} + \frac{\delta\prime(\tau)}{c_p}\right\}$$

$$-\frac{Rbe^{-bt}}{4\pi c_p^2}\left\{\frac{b\delta(\tau)}{2R} - \frac{2I_1(ba)u(\tau)}{a^3 c_p} + \frac{bI_0(ba)u(\tau)}{a^2 c_p}\right\} \quad (25)$$

where $\delta\prime(\cdot)$ is the derivative of Dirac delta function and $I_0(\cdot)$ the zeroth-order modified Bessel function of the first kind.

For $d = 4$ [15], the integral in (22) is given by

$$\begin{aligned}
\tilde{F}_p^0 &= [Y(e^{-y}-1) - 12y + 24y^2 - 22y^3 + 12y^4]x \\
\tilde{F}_p^1 &= [Y(e^{-2y} - 5e^{-y} + 4) + 36y - 60y^2 + 36y^3]x \\
\tilde{F}_p^2 &= [Y(e^{-3y} - 5e^{-2y} + 10e^{-y} - 6) - 36y + 48y^2 - 18y^3]x \\
\tilde{F}_p^3 &= [Y(e^{-4y} - 5e^{-3y} + 10e^{-2y} - 10e^{-y} + 4) \\
&\quad + 12y - 12y^2 + 4y^3]x \\
\tilde{F}_p^4 &= Y(e^{-y} - 1)^5 x \\
\tilde{F}_p^k &= e^{-y}\tilde{F}_p^{k-1}, k > 4
\end{aligned} \quad (26)$$

Here, $y = \Delta t \sigma_p / \varepsilon_p$, $x = \varepsilon_p^3/(12\Delta t^4 \sigma_p^4)$, and $Y = -12 + 18y - 11y^2 + 3y^3$.

References

[1] H. Bagci, A. Yilmaz, J.-M. Jin, and E. Michielssen, "Fast and rigorous analysis of EMC/EMI phenomena on electrically large and complex cable-loaded structures," *IEEE Trans. Electromagn. Compat.*, vol. 49, no. 2, pp. 361–381, May 2007.

[2] E. Schlemmer, W. Rucker, and K. Richter, "Boundary element computations of 3D transient scattering from lossy dielectric objects," *IEEE Trans. Magn.*, vol. 29, no. 2, pp. 1524–1527, Mar. 1993.

[3] A. Yilmaz, D. S. Weile, B. Shanker, J.-M. Jin, and E. Michielssen, "Fast analysis of transient scattering in lossy media," *IEEE Antennas Wireless Propag. Lett.*, vol. 1, pp. 14–17, 2002.

[4] P.-L. Jiang and E. Michielssen, "Multilevel plane wave time domain-enhanced MOT solver for analyzing electromagnetic scattering from objects residing in lossy media," in *Proc. IEEE Int. Symp. Antennas Propag.*, Jul. 2005, vol. 3B, pp. 447–450.

[5] P.-L. Jiang and E. Michielssen, "Temporal acceleration of time-domain integral-equation solvers for electromagnetic scattering from objects residing in lossy media," *Microw. Opt. Technol. Lett.*, vol. 44, no. 3, pp. 223–230, 2005.

[6] C. Yang and V. Jandhyala, "Modeling of lossy multiregion substrates in microelectronic circuits using time-domain surface integral equations," *Microw. Opt. Technol. Lett.*, vol. 47, no. 1, pp. 68–73, 2005.

[7] P. M. Morse and H. Feshbach, *Methods of Theoretical Physics*. New York, NY, USA: McGraw-Hill, 1953.

[8] W. Chew, *Waves and Fields in Inhomogenous Media*, ser. IEEE Press Series on Electromagnetic Wave Theory. New York, NY, USA: Wiley, 1999.

[9] S. Rao, D. Wilton, and A. Glisson, "Electromagnetic scattering by surfaces of arbitrary shape," *IEEE Trans. Antennas Propag.*, vol. AP-30, no. 3, pp. 409–418, May 1982.

[10] G. Manara, A. Monorchio, and R. Reggiannini, "A space-time discretization criterion for a stable time-marching solution of the electric field integral equation," *IEEE Trans. Antennas Propag.*, vol. 45, no. 3, pp. 527–532, Mar. 1997.

[11] H. Bagci, A. Yilmaz, and E. Michielssen, "An FFT-accelerated time-domain multiconductor transmission line simulator," *IEEE Trans. Electromagn. Compat.*, vol. 52, no. 1, pp. 199–214, Feb. 2010.

[12] K. Donepudi, J.-M. Jin, and W. C. Chew, "A higher order multilevel fast multipole algorithm for scattering from mixed conducting/dielectric bodies," *IEEE Trans. Antennas Propag.*, vol. 51, no. 10, pp. 2814–2821, Oct. 2003.

[13] B. Shanker, A. A. Ergin, and E. Michielssen, "Plane-wave-time-domain-enhanced marching-on-in-time scheme for analyzing scattering from homogeneous dielectric structures," *J. Opt. Soc. Amer. A*, vol. 19, pp. 716–726, Apr. 2002.

[14] J. Bor, O. Lafond, H. Merlet, P. Le Bars, and M. Himdi, "Foam based Luneburg lens antenna at 60 GHz," *Prog. Electromagn. Res. Lett.*, vol. 44, pp. 1–7, 2014.

[15] H. Bagci, A. Yilmaz, V. Lomakin, and E. Michielssen, "Fast solution of mixed-potential time-domain integral equations for half-space environments," *IEEE Trans. Geosci. Remote Sens.*, vol. 43, no. 2, pp. 269–279, Feb. 2005.